Pushing the Performance Limits of Long Wavelength Interband Cascade Lasers using Innovative Quantum Well Active Regions

Yixuan Shen,[1] J. A. Massengale,[1] Rui Q. Yang[1,*], S. D. Hawkins[2], A. J. Muhowski[2]

[1]School of Electrical and Computer Engineering, University of Oklahoma, Norman, OK 73019, USA

[2]Sandia National Laboratories, PO Box 5800, Albuquerque, NM 87185-1085, USA

*email: Rui.q.Yang@ou.edu

Abstract

We report significantly enhanced device performance in long wavelength interband cascade lasers (ICLs) by employing a recently proposed innovative quantum well (QW) active region containing strained InAsP layers. These ICLs were able to operate at wavelengths near 14.4 μm, the longest ever demonstrated for III-V interband lasers, implying great potential of ICLs to cover an even wider wavelength range. Also, by applying the aforesaid QW active region configuration on ICLs at relatively short wavelengths, ICLs were demonstrated at a low threshold current density (*e.g.*, 13 A/cm^2 at 80 K) and at temperatures up to 212 K near 12.4 μm, more than 50K higher than the previously reported ICLs with the standard W-shape QW active region at similar wavelengths. This suggests that the QW active region with InAsP layers can be used to improve device performance at the shorter wavelengths.

Index Terms—III-V materials, advanced waveguide, Interband cascade laser (ICL), long wavelength operation, mid-IR laser, semiconductor laser.

Interband cascade lasers (ICLs) [1-2] based on type-II quantum wells (QWs) are an efficient mid-infrared light source for many practical applications due in large part to their low power consumption [2-11]. High performance operation of ICLs has been demonstrated at room temperature across a wavelength range from 2.7 μm to about 6 μm [2-8]. By using a plasmon waveguide on an InAs substrate for ICLs [12], pulsed lasing up to 55 °C near 7.1 μm was achieved [13]. However, extending the operation of ICLs to longer wavelengths with similar performance as their short wavelength counterparts is challenging due to factors such as the reduced wavefunction overlap in the type-II QW and the increased free-carrier absorption loss. For the commonly used W-shape type-II QW active region [14] with the conventional waveguide, the longest lasing wavelength achieved was 9.5 μm for an optically pumped laser [15]. By introducing a plasmon waveguide configuration, InAs-based ICLs exhibited elevated long wavelength (LW) operation up to 11.2 μm [16]. With the development of an advanced waveguide [17] that includes hybrid cladding layers, the operation was extended to 11.5 μm [18]. However, the maximum pulsed operating temperature for these LW ICLs using the plasmon and advanced waveguides was limited to 137 K at 11.5 μm, 155 K at 11.2 μm [18], and 190 K at 10.4 μm [19], which is much lower than their short wavelength counterparts. As the lasing wavelength increases, the device performance of these LW ICLs degrades dramatically, partly due to the reduced electron-hole wavefunction overlap in the type-II QW. To alleviate this issue, we have recently proposed and implemented an innovative QW active region in LW ICLs utilizing $InAs_{0.5}P_{0.5}$ barriers [18, 20]. Based on the perspective of band structure [21], these $InAs_{0.5}P_{0.5}$ barriers can lower the interband transition energy, facilitating lasing at longer wavelengths with reduced InAs layer thicknesses. Indeed, the initial ICLs with $InAs_{0.5}P_{0.5}$ barriers in the QW active region showed a pulsed lasing wavelength beyond 13 μm [20], with an operating temperature up to 160 K at 12.97 μm and 150 K at 13.1 μm [18]. These preliminary results indicate a promising approach to expanding the frontiers of LW ICLs.

In this work, using the above-mentioned QW active region containing strained $InAs_{0.5}P_{0.5}$ layers, we demonstrated not only a substantial expansion of the wavelength coverage of ICLs to nearly 14.4 μm, the longest ever reached for III-V interband lasers, but also significantly enhanced device performance in terms of reduced threshold current density (*e.g.*, 13 A/cm^2 at 80 K) and increased operating temperature up to 212 K near 12.4 μm. These achievements suggest an extraordinary potential for ICLs to cover an even wider wavelength range in the future, and to improve device performance with higher operating temperatures at shorter wavelengths.

Three ICL wafers (EB7904, EB7906, and EB7908) were grown by MBE on InAs substrates, all of which incorporated the advanced waveguide [17-18] and featured the $InAs_{0.5}P_{0.5}$ barriers in the QW active region. ICL wafers EB7904 (EB7906) are composed of 23 cascade stages with an active region layer sequence of $AlAs_{0.89}Sb_{0.11}$/$InAs_{0.5}P_{0.5}$/InAs/$Ga_{0.65}In_{0.35}Sb$/InAs/$InAs_{0.5}P_{0.5}$, with thicknesses of 19/16/25/28/20/16(13) Å in the growth direction. ICL wafer EB7908 had a similar active region design, but with 20 cascade stages and reduced InAs layer thicknesses in the W-QW active region of 21 Å and 17 Å. This was done in order to evaluate this modified QW for shorter wavelength operation near 11 μm, comparable to that of ICLs with the regular W-QW active region reported in Ref. 18. All three ICL wafers have the same electron and hole injector regions.

Compared to the ICLs in Ref. 18, the GaSb layer thicknesses in the hole injector were increased by ~10% to raise the hole energy levels towards the valence band edge of GaSb so that the interband tunneling window can be enlarged [21] at a given voltage, facilitating more efficient carrier transport with a reduced threshold voltage [22]. Additionally, for EB7904 and EB7906, the doping concentrations in the electron injectors and n^+-InAs cladding layers were reduced to 7.3×10^{17}/cm^3 and 2.5×10^{18}/cm^3 to minimize free-carrier absorption, respectively, while the thicknesses of the InAs separate confinement layer (SCL) and superlattice (SL) intermediate cladding layer were increased to 1.15 and 1.9 μm, respectively, to accommodate the long wavelength (~13 μm) photons. Pieces of the wafers were fabricated into 100-μm-wide and 150-μm-wide broad area (BA) mesas using standard UV contact photolithography and wet chemical etching. They were left unthinned and

cleaved into approximately 1.5-mm-long laser bars without facet coating, which were mounted epi-side up on copper heat sinks for testing.

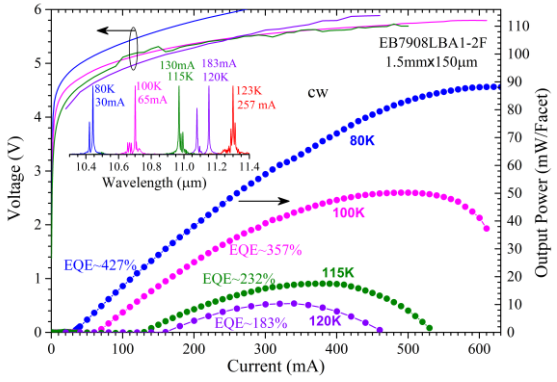

Fig.1. Current-voltage-light (IVL) characteristics in cw mode of an ICL from wafer EB7908, with its lasing spectra (inset).

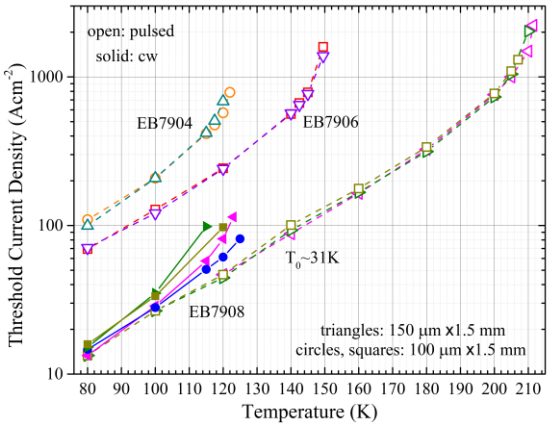

Fig. 2. Threshold current density as a function of temperature for ICLs made from three wafers.

A 150-μm-wide ICL from EB7908 lased in continous wave (cw) up to 123 K with a lasing wavelength near 11.3 μm, red-shifted from 10.45 μm at 80 K, as shown in Fig. 1. The threshold current density J_{th} for this device is 13 A/cm^2 at 80 K, similar to that from a previously reported ICL with the W-shape QW active region near 10.2 μm, but significantly lower than 26.7A/cm^2 for another ICL near 10.9 μm [18]. Their external quantum efficiencies (EQEs) are comparable, but the output power of this device reached 89 mW/facet at 80 K, as shown in Fig. 1. This output power is much higher than the previously reported maximum value of 56 mW/facet at a somewhat shorter wavelength [18]. This could be partially because ICLs with InAsP barriers can operate at a much higher current density than ICLs with the regular QW active region in this LW range, which is also true for pulsed operation, as will be presented below. Similar performance was observed from multiple devices made from EB7908. For example, a 100-μm-wide ICL lased in cw at temperatures up to 125 K with an output power of 8 mW/facet and an EQE of 115% and delivered a maximum output power of 80 mW/facet at 80 K with an EQE of 452%. Their threshold current densities are summarized in Fig. 2. The threshold voltage V_{th} was about 5.1 to 5.3 V at 80 K, corresponding to a voltage efficiency from 47% to 45%, which is substantially improved from 31%-35% for the initial ICLs with InAsP barriers [18]. However, it is still substantially less than the voltage efficiency of ~80% observed in early InAs-based ICLs [5], suggesting room for further improvement.

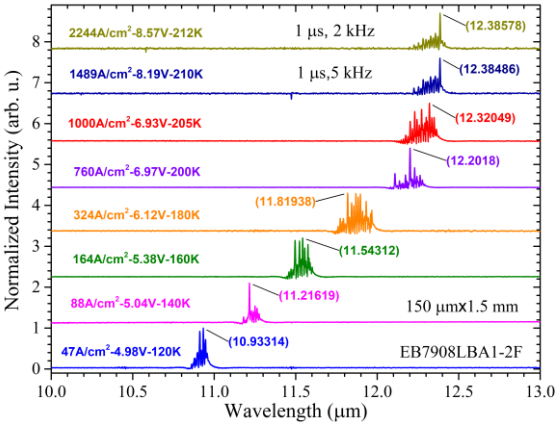

Fig. 3. Pulsed lasing spectra of an ICL from EB7908.

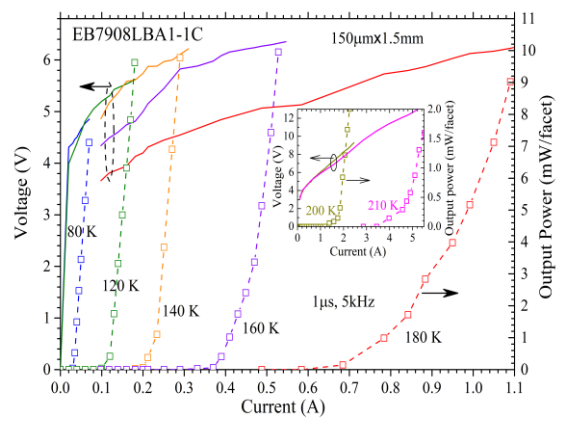

Fig. 4. Pulsed IVL of an ICL from EB7908.

In the pulsed mode with 1 μs current pulses at 5 kHz (2 kHz for temperatures at 212 K to reduce the heating), the device in Fig. 1 lased at temperatures up to 212 K near 12.4 μm as shown in Fig. 3, which is 57 K higher than the maximum operating temperature of a previous ICL at a similar wavelength [18]. Again, compared to the previous ICLs with the regular W-shape QW active region at similar wavelengths, the operating current allowed in this device is much higher and consequently could afford a threshold current density of ~2244 A/cm^2 at 212 K. Its pulsed threshold current density at various temperatures is plotted in Fig. 2, from which a characteristic temperature T_0 of 31 K is extracted, which is comparable with previous ICLs at similar wavelengths [18] but covers a relatively wider temperature range. From the current-voltage-light (IVL) characteristics of a BA ICL, as shown in Fig. 4, the slope efficiency was nearly unchanged from 80 K to 160 K in pulsed operation and then decreased rapidly at higher temperatures, but it could still deliver a few milliwatts per facet of peak power.

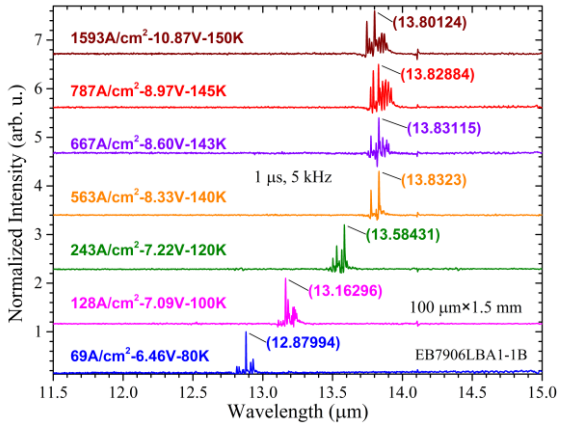

Fig. 5. Pulsed spectra of an ICL from EB7906.

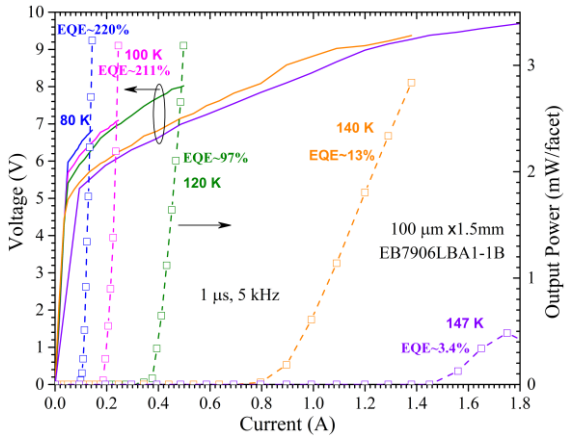

Fig. 6. Pulsed IVL of an ICL from EB7906.

In the pulsed mode, the ICLs from EB7906 lased at temperatures up to 150 K near 13.8 μm, as shown in Fig. 5, which is noticeably longer than the reported 13.1 μm in Ref. 18 with a similar QW active region due possibly to variations in the layer thicknesses with changing growth conditions over time. At these longer wavelengths, the threshold current density was 69 A/cm^2 at 80 K to 1593 A/cm^2 at 150 K, as shown in Fig. 5 and Fig. 2 for two devices from EB7906. Because of the longer wavelength, the J_{th} was somewhat higher than that for the 13.1 μm ICL in Ref. 18. However, their maximum operating temperatures are the same, which is mainly attributed to the newer ICL having more cascade stages (23 vs 20) and the modified design with reduced doping concentrations and increase thicknesses of SCL and cladding layers in EB7906. Nevertheless, the threshold voltage was also higher (*e.g.*, 6.46 V at 80 K, corresponding to a voltage efficiency of 34%) with more cascade stages. Consequently, heating was more serious so that the cw operation was not achieved in BA devices from EB7906. They were able to be operated in quasi-cw mode at 5-20% duty cycle with multiple milliwatts of average output power, from which reliable EQE were extracted for the device in pulsed operation, as shown in Fig. 6. Even at this long wavelength, the device had an EQE exceeding 200% at 80 and 100 K, which dropped quickly when the temperature was raised above 120 K. The EQE at 80 K was lower than previously reported values (>300%) for early ICLs at

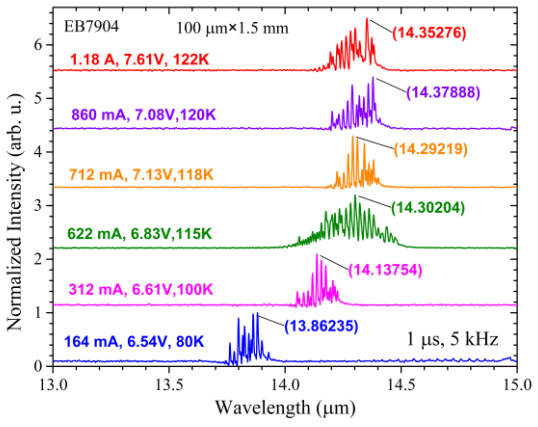

Fig. 7. Pulsed spectra of an ICL from EB7904.

relatively short wavelengths (11.8- 12.1 μm) [18], but much higher than the reported 41% for the initial ICL with the InAsP barrier layers and emission wavelength of 12.7 μm at 80 K [20], suggesting that the optical internal absorption loss was decently controlled at low temperatures and at such a long wavelength (12.9 μm).

The ICLs from EB7904 lased in pulsed mode at temperatures up to 122 K near 14.35 μm, as shown in Fig. 7, red-shifted from 13.86 μm at 80 K and slightly blue-shifted from 14.38 μm at 120 K due possibly to the band-filling effect. Compared to ICLs from EB7906, the actually grown layers might be slightly thicker, and the designed 16 Å InAsP layer (near the hole injector) is 3 Å thicker than that in EB7906, which contributed to the longer lasing wavelength. With significantly increased wavelengths, the threshold current density was higher and increased from 109 A/cm^2 at 80 K to 787 A/cm^2 at 122 K, as shown in Fig. 2. At 80 K, the threshold voltage was 6.54 V, corresponding to a voltage efficiency of 31%, similar to that in devices from EB7906. This low voltage efficiency could still be related to possible carrier transport issues in addition to a substantial voltage drop on parasitic resistance with a relatively high threshold current, which will be a subject of further research.

In summary, significantly enhanced device performance of LW ICLs has been demonstrated by utilizing modified QW active regions compared to the commonly used W-shape QWs, which pushed the wavelength coverage beyond 14 μm, suggesting exceptional potential and capability of ICLs to operate in an even wider range in the mid-infrared region. Also, the modification of the QW active region can substantially improve device performance towards the high temperature operation with shorter wavelengths. In combining other quantum engineering techniques such as mitigating inter-valence-subband transition absorption loss [7-8], further improvements in device performance of ICLs are expected at LWs and the shorter wavelengths (e.g., 8-10 μm) in the future. It is noteworthy that although excellent device performance was achieved at 80 K, these ICLs are far from room temperature operation compared to quantum cascade lasers in this LW (12-15 μm) region [23]. Continued effort and innovations will be required to push them towards operation at room temperature and above for many practical applications.

Acknowledgement: The work at the University of Oklahoma was partially supported by NSF (No. ECCS-1931193). This work was performed, in part, at the Center for Integrated Nanotechnologies, an Office of Science User Facility operated for the U.S. Department of Energy (DOE) Office of Science. This article has been authored by an employee of National Technology & Engineering Solutions of Sandia, LLC under Contract No. DE-NA0003525 with the U.S. Department of Energy (DOE). The employee owns all right, title and interest in and to the article and is solely responsible for its contents. The United States Government retains and the publisher, by accepting the article for publication, acknowledges that the United States Government retains a non-exclusive, paid-up, irrevocable, world-wide license to publish or reproduce the published form of this article or allow others to do so, for United States Government purposes. The DOE will provide public access to these results of federally sponsored research in accordance with the DOE Public Access Plan https://www.energy.gov/downloads/doe-public-access-plan. We thank Zhisheng Shi for lending a MCT detector used for the pulsed power testing.

Author Contributions

Y. Shen: Investigation (equal); Data curation (lead); Writing – original draft (supporting); Writing – review & editing (equal); **J. A. Massengale**: Investigation (equal); Data curation (equal); Writing – original draft (supporting); Writing – review & editing (equal); **R. Q. Yang**: Conceptualization (lead); Investigation (supporting); Writing – original draft (lead); Writing – review & editing (equal); **S. D. Hawkins**: Investigation (equal); Writing – review & editing (supporting); **A. J. Muhowski**: Investigation (equal); Writing – review & editing (equal).

Data availability

The data are available from the corresponding author upon reasonable request.

REFERENCES

[1] R. Q. Yang, "Infrared laser based on intersubband transitions in quantum wells", *Superlattices Microstruct*., **17**, 77 (1995).

[2] R. Q. Yang, "Interband Cascade (IC) Lasers," in *Semiconductor Lasers fundamentals and applications*, edited by A. Baranov and E. Tournie, Cambridge, UK: Woodhead Publishing, 2013, ch. 12, pp. 487-513.

[3] I. Vurgaftman, R. Weih, M. Kamp, J. R. Meyer, C. L. Canedy, C. S. Kim, M. Kim, W. W. Bewley, C. D. Merritt, J. Abell, "Interband Cascade Lasers," J. Phys. D: Appl. Phys. **48** 123001 (2015).

[4] J. Koeth, R. Weih, J. Scheuermann, M. Fischer, A. Schade, M. Kamp, S. Höfling, "Mid infrared DFB interband cascade lasers", Proc. SPIE, **10403**, 1040308 (2017).

[5] R. Q. Yang, L. Li, W. Huang, S. M. Shazzad Rassel, J. A. Gupta, A. Bezinger, X. Wu, G. Razavipour, and G. C. Aers, "InAs-based interband cascade lasers", *IEEE J. Sel. Top. Quant. Electron*., **25**, 1200108 (2019).

[6] J. R. Meyer, W. W. Bewley, C. L. Canedy, C. S. Kim, M. Kim, C. D. Merritt, and I. Vurgaftman, "The interband cascade laser", *Photonics*, **7**, 75 (2020).

[7] H. Knotig, J. Nauschutz, N. Opacak, S. Hofling, J. Koeth, R. Weih, and B. Schwarz, "Mitigating valence intersubband absorption in interband cascade lasers", Laser & Photonics Reviews, 2200156 (2022).

[8] J. Nauschutz, H. Knotig, R. Weih, J. Scheuermann, J. Koeth, S. Hofling, and B. Schwarz, "Pushing the room temperature continuous-wave operation limit of GaSb-based interband cascade lasers beyond 6 μm", Laser & Photonics Reviews, 2200587 (2023).

[9] C. S. Goldenstein, R. M. Spearrin, J. B. Jeffries, and R. K. Hanson, "Infrared laser-absorption sensing for combustion gases," Prog. Energy Combust. Sci. **60**, 132 (2017).

[10] J. Scheuermann, P. Kluczynski, K. Siembab, M. Straszewski, J. Kaczmarek, et al, "Interband Cascade Laser Arrays for Simultaneous and Selective Analysis of C1–C5 Hydrocarbons in Petrochemical Industry", Applied Spectroscopy **75** (3), 336 (2021).

[11] P. Didier, H. Knötig, O. Spitz, L. Cerutti, A. Lardschneider, E. Awwad, D. Diaz-Thomas, A. N. Baranov, R. Weih, J. Koeth, B. Schwarz, and F. Grillot, "Interband cascade technology for energy-efficient mid-infrared free-space communication," Photon. Res. **11**, 582 (2023).

[12] Z. Tian, R. Q. Yang, T. D. Mishima, M. B. Santos, R. T. Hinkey, M. E. Curtis, and M. B. Johnson, "InAs-based interband cascade lasers near 6 μm", Electron. Lett. **45**, 48 (2009).

[13] M. Dallner, F Hau, S Höfling, M Kamp, "InAs-based interband cascade lasers emitting around 7 μm with threshold current densities below 1 kA/cm^2 at room temperature", Appl. Phys. Lett., **106**, 041108 (2015).

[14] J.R. Meyer, C.A. Hoffman, F.J. Bartoli, L.R. Ram-Mohan, "Type-II quantum-well lasers for the mid-wavelength infrared", Appl. Phys. Lett., **67**, 757 (1995).

[15] A. P. Ongstad, R. Kaspi, G. C. Dente, M. L. Tilton, R. Barresi, and J. R. Chavez, "Wavelength tuning limitations in optically pumped type-II antimonide lasers", *Appl. Phys. Lett.*, **92**, 141106 (2008).

[16] L. Li, H. Ye, Y. Jiang, R. Q. Yang, J. C. Keay, T. D. Mishima, M. B. Santos, and M. B. Johnson, "MBE-grown long-wavelength interband cascade lasers on InAs substrates", *Journal of Crystal Growth,* **425**, 369 (2015).

[17] L. Li, Y. Jiang, H. Ye, R. Q. Yang, T. D. Mishima, M. B. Santos, and M. B. Johnson, "Low-threshold InAs-based interband cascade lasers operating at high temperatures", *Appl. Phys. Lett*., **106**, 251102 (2015).

[18] J. A. Massengale, Y. Shen, R. Q. Yang, S. D. Hawkins, and J. F. Klem, "Enhanced Performance of InAs-based Interband Cascade Lasers Emitting between 10-13 μm," Semiconductor Science and Technology **38**, 025009 (2022).

[19] Z. Tian, L. Li, H. Ye, R.Q. Yang, T.D. Mishima, M.B. Santos, and M.B. Johnson, "InAs-based interband cascade lasers with emission wavelengths at 10.4 μm," *Electron. Lett*. **48**, 113–114 (2012).
[20] J. A. Massengale, Y. Shen, R. Q. Yang, S. D. Hawkins, and J. F. Klem, "Long wavelength interband cascade lasers," Appl. Phys. Lett. **120**, 091105 (2022).
[21] R. Q. Yang, "Electronic States and Interband Tunneling Conditions in Type-II Quantum Well Heterostructures", J. Appl. Phys. **127**, 025705 (2020).
[22] J. A. Massengale, Y. Shen, R. Q. Yang, S. D. Hawkins, and A. J. Muhowski, "Low threshold, long wavelength interband cascade lasers with high voltage efficiencies," (to be published).
[23] A. N. Baranov, M. Bahriz, and R. Teissier, "Room temperature continuous wave operation of InAs-based quantum cascade lasers at 15 μm," Opt. Express **24**, 18799 (2016).